Illustrations of Physical Bounds on Non-Dipole Radiators

Marius Cismasu and Mats Gustafsson
Dept. of Electrical and information technology, Lund University, Lund, Sweden.
{*marius.cismasu, mats.gustafsson*}*@eit.lth.se*

Abstract
Applications of physical bounds for radiator structures can be used to derive a priori estimates for antenna parameters in terms of directivity-bandwidth product. These estimates relate the static electric and magnetic polarizability properties of the radiating structure to its dynamic features. Highly electrically polarizable structures are analyzed numerically. Electric polarizability is computed using a Method of Moments (MoM) code and, based on it, the physical bounds are expressed. The realized parameters of the structures, computed using commercial electromagnetic simulators, are then compared with the bounds to show very good agreement.

1. INTRODUCTION

The physical bounds on antennas, described in [1–4], relate the performance of the antenna to the electrostatic and magnetostatic polarizabilities of its geometry and the generalized absorption efficiency. This approach is a generalization of Chu's classical bounds for spherical geometries [5] to geometries of arbitrary shape.

The generalized (or all spectrum) absorption efficiency is the only parameter in the bound related to the dynamic properties of the antenna. Minimum scattering is a well known property that many small matched antennas have; based on this property it is demonstrated that η is close to $1/2$ for many small antennas connected to a frequency independent resistive load (see [1–4]).

Here it is shown that we obtain good estimates for antenna parameters from the static polarizability of the radiating structure. Only electrically highly polarizable antennas are analyzed.

2. PHYSICAL BOUNDS

2.1. Theory

A number of previous articles have been dedicated to establishing a solid base for expressing physical bounds in engineering terms, [1–4]. We consider in the following that we are analyzing single port, linearly polarized, reciprocal and lossless antennas; denote the reflection coefficient $\Gamma(k)$ and the directivity $D(k;\hat{\boldsymbol{k}},\hat{\boldsymbol{e}})$, where k is the free-space wavenumber, $\hat{\boldsymbol{k}}$ the specific direction of radiation and $\hat{\boldsymbol{e}}$ the electric polarization. The sum rule derived in [1] gives the antenna identity

$$\int_0^\infty \frac{(1-|\Gamma(k)|^2)D(k;\hat{\boldsymbol{k}},\hat{\boldsymbol{e}})}{k^4}\,\mathrm{d}k = \frac{\eta}{2}\left(\hat{\boldsymbol{e}}\cdot\gamma_\mathrm{e}\cdot\hat{\boldsymbol{e}}+(\hat{\boldsymbol{k}}\times\hat{\boldsymbol{e}})\cdot\gamma_\mathrm{m}\cdot(\hat{\boldsymbol{k}}\times\hat{\boldsymbol{e}})\right), \quad (1)$$

where γ_e and γ_m are the electrostatic and magnetostatic polarizability dyadics, respectively.

Bounding the integral (1) in various ways produces relations for different applications. The resonant case, described in detail in [3], can be used when the antenna's behavior shows a dominant resonance in the partial realized gain and gives the following:

$$\frac{D(k_0;\hat{\boldsymbol{k}},\hat{\boldsymbol{e}})}{Q} \leq \leq \frac{\eta k_0^3}{2\pi}\left(\hat{\boldsymbol{e}}\cdot\gamma_\mathrm{e}\cdot\hat{\boldsymbol{e}}+(\hat{\boldsymbol{k}}\times\hat{\boldsymbol{e}})\cdot\gamma_\mathrm{m}\cdot(\hat{\boldsymbol{k}}\times\hat{\boldsymbol{e}})\right), \quad (2)$$

where k_0 is the resonance wavenumber and Q is the quality factor at the resonance. Most of the usual narrow band radiators show a dominant resonance which is the first resonance frequency.

The electric polarizability dyadic is evaluated for perfect electric conductors (see [1, 6]) to the high contrast polarizability dyadic, γ_∞ (because the electric susceptibility dyadic is infinitely large for PEC). The same result is obtained for any electric material if a conductivity term is present in its susceptibility dyadic, regardless of other material parameters, *cf.*, [7]. Assuming that magnetic polarizability has negligible influence – usually negative value for PEC – for electric antennas with linear polarization, we rewrite 2 as:

$$\frac{D(k_0;\hat{\boldsymbol{k}},\hat{\boldsymbol{e}})}{Q} \leq \frac{\eta k_0^3}{2\pi}(\hat{\boldsymbol{e}}\cdot\gamma_\infty\cdot\hat{\boldsymbol{e}}). \quad (3)$$

The above equation shows that an immediate upper bound estimation for the performance parameters D and Q of an electric antenna derives from the static electric polarizability. The latter parameter is usually much easier to compute than the directivity of the antenna and this is the advantage of 3. Furthermore, in order to directly compare the performance of different antennas we

normalize 3 to the value obtained for the smallest circumscribing sphere, *i.e.*, we divide by $k_0^3 a^3$:

$$\frac{D(k_0;\hat{\boldsymbol{k}},\hat{\boldsymbol{e}})}{Qk_0^3a^3} \leq \frac{\eta}{2\pi a^3}(\hat{\boldsymbol{e}}\cdot\gamma_\infty\cdot\hat{\boldsymbol{e}}), \tag{4}$$

where a is the the radius of the smallest circumscribed sphere to the antenna geometry.

There are two things that have to be accounted for when using the above results. The first one is to verify that the radiator has a generalized absorption efficiency of 1/2. The second one is to evaluate whether the influence of the magnetic polarizability on the results is negligible or not. These two effects can be verified at the same time using a broadband scattering analysis of the radiator.

Considering a plane wave of polarization $\hat{\boldsymbol{e}}$ impinging in direction $\hat{\boldsymbol{k}}$ on the analyzed antenna, the generalized absorption efficiency is defined as (see [3]):

$$\eta(\hat{\boldsymbol{k}},\hat{\boldsymbol{e}}) = \frac{\int_0^\infty \sigma_{\mathrm{a}}(k;\hat{\boldsymbol{k}},\hat{\boldsymbol{e}})/k^2\mathrm{d}k}{\int_0^\infty \frac{\sigma_{\mathrm{ext}}(k;\hat{\boldsymbol{k}},\hat{\boldsymbol{e}})}{k^2}\mathrm{d}k}, \tag{5}$$

where σ_{a} is the absorption cross section (or the effective antenna aperture) and σ_{ext} is the extinction cross section. The denominator of the previous equation is called the integrated extinction cross section ($\int \sigma_{\mathrm{ext}}$) and it is related to the antenna characteristics by:

$$\int_0^\infty \frac{\sigma_{\mathrm{ext}}(k;\hat{\boldsymbol{k}},\hat{\boldsymbol{e}})}{k^2}\mathrm{d}k = \frac{\pi}{2}\left(\hat{\boldsymbol{e}}\cdot\gamma_{\mathrm{e}}\cdot\hat{\boldsymbol{e}} + (\hat{\boldsymbol{k}}\times\hat{\boldsymbol{e}})\cdot\gamma_{\mathrm{m}}\cdot(\hat{\boldsymbol{k}}\times\hat{\boldsymbol{e}})\right), \tag{6}$$

By computing 6 and comparing with 4 it is possible to estimate the influence of the magnetic polarizability on the result. Note that in the view of the plane wave scattering on the structure, the bounds will read:

$$\frac{D(k_0;\hat{\boldsymbol{k}},\hat{\boldsymbol{e}})}{Qk_0^3a^3} \leq \frac{\eta(-\hat{\boldsymbol{k}},\hat{\boldsymbol{e}})}{2\pi a^3}(\hat{\boldsymbol{e}}\cdot\gamma_\infty\cdot\hat{\boldsymbol{e}}), \tag{7}$$

saying that if the directivity in one direction of the space is inserted into the bounds, then verification should be carried out by considering a plane wave impinging from that direction, thus the minus sign.

2.2. Implementation

The above theoretical results have been rigorously proven and verified. They have not yet been used as estimators for real structures' performance. In the real life applications, one should start by analyzing the chosen geometry. This is done by computing the right hand side of 4 using $\eta = 1/2$ and the electric polarizability computed for the structure:

$$\frac{\eta}{2\pi a^3}(\hat{\boldsymbol{e}}\cdot\gamma_\infty\cdot\hat{\boldsymbol{e}}) \approx \frac{0.5\cdot\gamma_c}{2\pi a^3}, \tag{8}$$

where $\gamma_c = \hat{\boldsymbol{e}}\cdot\gamma_\infty\cdot\hat{\boldsymbol{e}}$ can be obtained by using a MoM code, to obtain γ_∞, and then computing the scalar product for the analyzed polarization.

Direct comparison can be made between the analyzed structure and a reference geometry. Reference geometry might be the geometry of the available space in the device, a circumscribed geometry or even the smallest circumscribing sphere. There are a number of geometries for which the high contrast polarizability can be expressed analytically; otherwise the reference geometry has to be analyzed with a MoM code to obtain its high contrast polarizability and then compute the scalar product to obtain γ_{cg}. The closer

$$\frac{\gamma_c}{\gamma_{cg}} \leq 1 \tag{9}$$

is to 1, the better the analyzed antenna performs compared to the chosen (optimal) reference geometry with respect to the D/Q value.

From an engineering point of view we are interested to see to what extent the theory agrees with the experiment. To do this we must simulate the structure as a transmitter antenna; here we use Efield[†] to compute the far field and obtain D. Note that D is computed in the direction of interest and considering only the analyzed linear polarization. The Q-factor is computed based on the impedance behavior around the resonance ([8,9]) as:

$$Q \approx \omega_0 \frac{Z_i'}{2R}, \tag{10}$$

where ω_0 is the angular frequency at the resonance, Z_i' is the first derivative of the structure's input impedance with respect to the angular frequency and $R = \mathrm{Re}\, Z_i$ is the real part of the input impedance at the resonance frequency.

We can now verify the bound 4 using the simplified right hand side in 8. The closer the realized D/Q value is to the bound, the better the antenna performs.

Further on, the assumptions made in 2.1should be verified. A scattering simulation is needed: the same structure analyzed before is now excited by a plane wave impinging from the direction and having the same polarization as the previously computed directivity. The extinction cross section is computed from the forward scattering dyadic, $\mathbf{S}(k;-\hat{\boldsymbol{k}},\hat{\boldsymbol{e}})$ (see [6]):

$$\sigma_{\mathrm{ext}}(k;-\hat{\boldsymbol{k}},\hat{\boldsymbol{e}}) = \frac{4\pi}{k}\,\mathrm{Im}\{\hat{\boldsymbol{e}}^*\cdot\mathbf{S}(k;-\hat{\boldsymbol{k}},\hat{\boldsymbol{e}})\cdot\hat{\boldsymbol{e}}\}. \tag{11}$$

[†] www.efieldsolutions.com

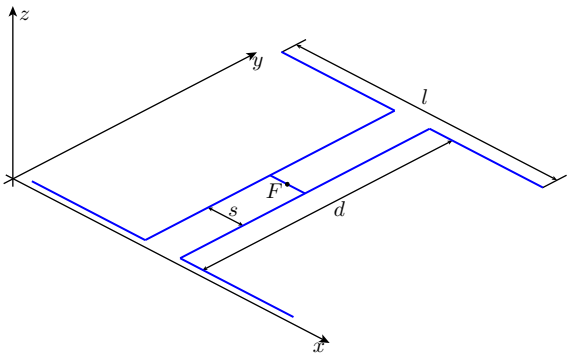

Fig. 1: Two dipole array.

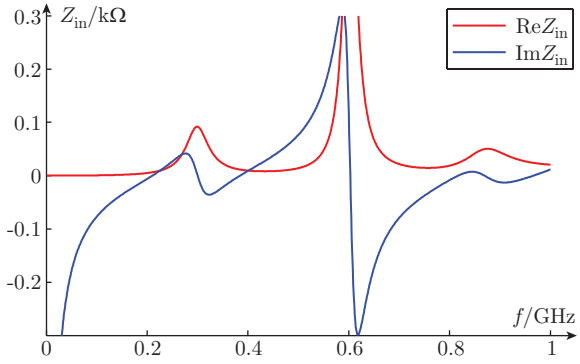

Fig. 2: Input impedance of the array in Fig. 1.

The absorption cross section is related to the directivity and feed mismatch, *cf.*, [3], and thus does not necessarily require the scattering simulation:

$$\sigma_{\text{a}}(k; -\hat{\boldsymbol{k}}, \hat{\boldsymbol{e}}) = \frac{\pi}{k^2} D(k; \hat{\boldsymbol{k}}, \hat{\boldsymbol{e}})(1 - |\Gamma(k)|^2). \quad (12)$$

The integrals under 5 can be evaluated numerically, thus the above functions must be defined in a large number of discrete frequencies. After this computation is performed, the assumption of $\eta \approx 1/2$ and $\left(\hat{\boldsymbol{e}} \cdot \gamma_{\text{e}} \cdot \hat{\boldsymbol{e}} + (\hat{\boldsymbol{k}} \times \hat{\boldsymbol{e}}) \cdot \gamma_{\text{m}} \cdot (\hat{\boldsymbol{k}} \times \hat{\boldsymbol{e}})\right) \approx \hat{\boldsymbol{e}} \cdot \gamma_{\infty} \cdot \hat{\boldsymbol{e}}$ can be verified.

2.3. Numerical Examples

Two simple arrays have been simulated and the results are presented in the following. They are designed according to the guidelines in [**?**].

2.31 Two Dipole Array

The first example is an array made of two simple half lambda dipoles. Feeding/loading point is F. The dimensions in Fig. 1 are: dipole length, $l = 509.5\,\text{mm}$, dipole spacing, $d = 470\,\text{mm}$ and feeding spacing, $s = 9.5\,\text{mm}$; this results in the radius of the smallest circumscribing sphere $a = 349\,\text{mm}$. All wires, dipoles and feeding structure, have the radius $R_{\text{w}} = 4\,\text{mm}$.

The MoM code used to compute the high contrast polarizability of the structure gives the value $\gamma_{c,xx} = 43.9 \cdot 10^{-3}\,\text{m}^3$. This value does not say anything by itself, so we compare it with the electric polarizability of a PEC sphere circumscribing the array: $\gamma_{cg,xx} = 4\pi a^3 = 535.6 \cdot 10^{-3}\,\text{m}^3$. This results in: $\gamma_{c,xx}/\gamma_{cg,xx} = 0.082$; in other words, the maximum attainable performance of this array in terms of D/Q is approximately 8 % of the performance of the optimum sphere.

Next we simulate the structure in transmission by connecting at point F a voltage gap. The feeding structure, as it is designed, does not radiate. Input impedance behavior is shown in Fig. 2. It shows the first resonance approximately at 210 MHz with the radiation resistance $R = 6\,\Omega$. At this frequency, the maximum partial directivity of the far field in the x polarization is $D = 2.3$ achieved in the broadside. Computing $Q = 10$ and $k_0 a = 1.54$ we get the left hand side of 4 as $D/Qk_0^3a^3 = 0.062$. We have all the data to express 4 in numbers: $0.062 \leq 0.082$.

Under the assumptions that $\eta \approx 0.5$ and the influence of the magnetic polarizability is negligible, the previously computed result shows that the antenna achieves 75.6 % of the optimal performance of this structure. This leads to the conclusion that there is room for improvement for such a structure.

The verification of the assumptions is done by impinging a plane wave on the structure, from the broadside (the direction of maximum radiation at the first resonance); the antenna is loaded at point F with a resistance $R = 6\,\Omega$. A number of 1000 frequency points evenly distributed between 1 MHz and 1 GHz were used to obtain $\eta = 0.46$ and $I\sigma_{\text{ext}} = 42.6 \cdot 10^{-3}\,\text{m}^3$. These figures show us that indeed the contribution of the magnetic polarization is negligible ($I\sigma_{\text{ext}}$ is less than 3% away from $\gamma_{c,xx} = 43.9 \cdot 10^{-3}\,\text{m}^3$ even though the integration interval is limited and small) and the antenna does not absorb as much power as it radiates at the dominating resonance. Thus we can say that the right hand side of 4 is $0.46 \cdot \gamma_c/2\pi a^3 = 0.075$ showing an antenna performing at 82 % of its optimum.

2.32 Four Dipole Array

The second example is a four dipole linear array depicted in Fig. 3. The dimensions are: $l = 500\,\text{mm}$, $d = 500\,\text{mm}$ and $s = 2.7\,\text{mm}$. The dipoles are connected via a transmission line made of two parallel wires. All wires have the same radius $R_{\text{w}} = 1\,\text{mm}$. The smallest circum-

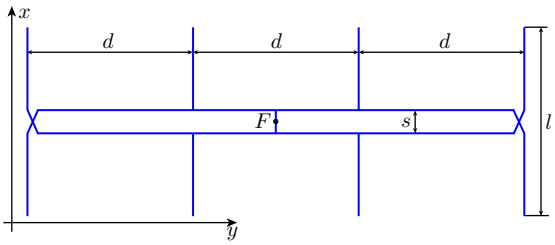

Fig. 3: Four dipole array.

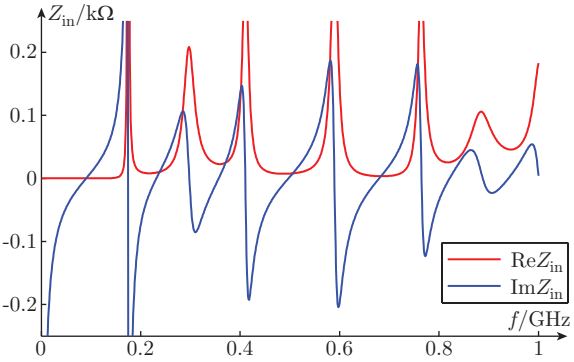

Fig. 4: Input impedance of the array depicted in Fig. 3.

scribing sphere to this structure has the radius $a = 792\,\text{mm}$.

The high contrast polarizability of this structure is $\gamma_{c,xx} = 57.5 \cdot 10^{-3}\,\text{m}^3$. Compared with its smallest circumscribing sphere $\gamma_{c,xx}/\gamma_{cg,xx} = 0.009$. Note that when comparing with the smallest circumscribed sphere, the previous ratio has the same value as the simplified bound in equation 8.

For the transmission simulation we connect a voltage gap at point F. In this way all the dipoles are in phase at the designed frequency. Fig. 4 shows the input impedance. The array has the first resonance with non-zero radiation resistance, $R = 9\,\Omega$, approximately at 232 MHz. Maximum partial directivity of the x polarization is $D = 6.3$ in the broadside. With $Q = 20$ and $k_0 a = 3.85$ we get $D/Qk_0^3a^3 = 0.006$ and $0.006 \leq 0.009$. This shows that the array achieves approximately 60 % of the optimum performance.

For verification we simulate the structure in plane wave excitation, impinging from broadside, at 1000 frequencies evenly distributed between 1 MHz and 1 GHz and with a load of $9\,\Omega$ connected at point F. The results are: $\eta = 0.42$ and $I\sigma_{\text{ext}} = 56.3 \cdot 10^{-3}\,\text{m}^3$. The deviation between the integrated extinction cross section and the polarizability of the structure is less than 2 %, so the influence of the magnetic polarizability is negligible and the absorption efficiency computed before is a realistic value. Under these circumstances the bound is decreased to 0.008 showing an array performing at more than 70 % of the optimum performance.

3. CONCLUSION

The well established bounds are applied to practical high directivity antennas. The agreement between theory and simulations is very good especially considering the fact that the antennas have not been optimized in any way.

Static electric polarizability properties of antennas can be used to compare their achievable performance in the first stage of the design process. These properties require very little computational effort as compared with the far field and input impedance computation. In this sense, the term expressed in 8 is the performance figure to be directly compared between different radiators.

4. ACKNOWLEDGMENTS

The support of the Swedish research council is gratefully acknowledged.

5. REFERENCES

[1] M. Gustafsson, C. Sohl, and G. Kristensson, "Physical limitations on antennas of arbitrary shape," *Proc. R. Soc. A*, vol. 463, pp. 2589–2607, 2007.

[2] C. Sohl and M. Gustafsson, "A priori estimates on the partial realized gain of Ultra-Wideband (UWB) antennas," *Quart. J. Mech. Appl. Math.*, vol. 61, no. 3, pp. 415–430, 2008.

[3] M. Gustafsson, C. Sohl, and G. Kristensson, "Illustrations of new physical bounds on linearly polarized antennas," *IEEE Trans. Antennas Propagat.*, vol. 57, no. 5, pp. 1319–1327, May 2009.

[4] A. Derneryd, M. Gustafsson, G. Kristensson, and C. Sohl, "Application of gain-bandwidth bounds on loaded dipoles," *IET Microwaves, Antennas & Propagation*, vol. 3, no. 6, pp. 959–966, 2009.

[5] L. J. Chu, "Physical limitations of omnidirectional antennas," *Appl. Phys.*, vol. 19, pp. 1163–1175, 1948.

[6] C. Sohl, M. Gustafsson, and G. Kristensson, "Physical limitations on broadband scattering by heterogeneous obstacles," *J. Phys. A: Math. Theor.*, vol. 40, pp. 11 165–11 182, 2007.

[7] R. E. Kleinman and T. B. A. Senior, "Rayleigh scattering," in *Low and high frequency asymptotics*, ser. Handbook on Acous-

tic, Electromagnetic and Elastic Wave Scattering, V. V. Varadan and V. K. Varadan, Eds. Amsterdam: Elsevier Science Publishers, 1986, vol. 2, ch. 1, pp. 1–70.

[8] M. Gustafsson and S. Nordebo, "Bandwidth, Q factor, and resonance models of antennas," *Progress in Electromagnetics Research*, vol. 62, pp. 1–20, 2006.

[9] A. D. Yaghjian and S. R. Best, "Impedance, bandwidth, and Q of antennas," *IEEE Trans. Antennas Propagat.*, vol. 53, no. 4, pp. 1298–1324, 2005.